Metals and Materials International (2018) 24:1293–1302
https://doi.org/10.1007/s12540-018-0146-z

Temperature-Dependent Thermal and Chemical Stabilities as well as Mechanical Properties of Electrodeposited Nanocrystalline Ni

Liangfu Zheng[1,2] · **Xiao Peng**[1,2]

Received: 7 December 2017 / Accepted: 9 May 2018 / Published online: 25 May 2018

Abstract
Nanocrystalline (NC) Ni electrodeposits (EDs) with a mean grain size of 34 ± 12 nm has been investigated, from room temperature to 800 °C under a purge gas of argon, by both non-isothermal and isothermal differential scanning calorimetry measurements, in combination with characterization of temperature-dependent microstructural evolution. A significant exothermic peak resulting from superimposition of recrystallization and surface oxidation occurs between 340 and 745 °C at a heating rate of 10 °C/min for the NC Ni EDs. The temperatures for recrystallization and oxidation increase with increasing the heating rate. In addition, recrystallization leads to a profound brittle–ductile transition of the Ni EDs in a narrow range around the peak temperature for the recrystallization.

Keywords Electron microscopy · Nickel alloys · Nanocrystalline materials · Thermal analysis · Hardness

1 Introduction

Nanocrystalline (NC) metallic materials with respect to conventional coarse-grained (normally micro-grained) polycrystalline counterparts display unique and generally improved physical, chemical, as well as mechanical properties, for example, higher thermal expansion coefficient, electrical resistivity and diffusivity, lower thermal conductivity, reduced density and elastic modulus, and increased hardness/strength, toughness/ductility, abrasion resistance and corrosion resistance [1–4]. However, because of the existence of a large proportion of high energy grain boundaries, NC materials relative to the perfect crystal store excess energy and thus become thermodynamically unstable. When exposed to high temperatures, they suffer dramatic changes in microstructure in terms of grain growth and recrystallization, which generally result in the degradation of the above-mentioned properties [5–11].

Nickel is widely used as a base metal in industrial processes. NC Ni was first fabricated by Erb et al. [12] in 1991 using electrochemical deposition, a technique with the merits of simple processing, ease of fabrication, low cost, high productivity, and good compositional control. Ni-based NC electrodeposits (EDs) have since been the model materials extensively studied for understanding thermal stability of NC metals. For examples, modulated differential scanning calorimetry (DSC) measurements indicated that the Ni EDs with a starting grain size of 20 nm emitted a thermal signal for grain growth at approximately 300 °C, releasing an enthalpy of 927.5 J/mol [13]. Using DSC and transmission electron microscopy (TEM), Wang et al. [14] found that the nanocrystals in Ni EDs were stable at temperatures below 280 °C but not thereafter with increasing temperature. The grains abnormally grew in size at temperatures over 280 °C with an activation energy of 135.1 kJ/mol, giving off an enthalpy of 415.7 ± 3.5 J/mol. Lin et al. [15] found that, due to the existence of a high density of dislocations and twins, Ni EDs recrystallized at temperatures higher than 300 °C and converted from the out-of-plane columnar grain structure into an equiaxed grain structure at 600 °C. However, a full explanation of the dependence of the DSC curves on the

Electronic supplementary material The online version of this article (https://doi.org/10.1007/s12540-018-0146-z) contains supplementary material, which is available to authorized users.

✉ Liangfu Zheng
lfzheng@alum.imr.ac.cn

✉ Xiao Peng
xpeng@imr.ac.cn

[1] School of Material Science and Engineering, Nanchang Hangkong University, Nanchang 330063, China

[2] Laboratory for Corrosion and Protection, Institute of Metal Research, Chinese Academy of Sciences, Shenyang 110016, China

microstructural evolution of NC Ni EDs at higher temperatures has still been lacking.

Recently, NC Ni EDs have been used as a base metal matrix, into which Cr and/or Al nanoparticles were simultaneously introduced during electrodeposition, for designing and developing coatings against oxidation at temperatures at or above 800 °C [16–18]. One characteristic of the advanced NC Ni-based coatings is that they have the ability to thermally grow a protective scale of either chromia or alumina at the Cr and/or Al contents obviously lower than normal level required by conventionally coarse-grained alloys [18–20]. This has been attributed to the fact that the NC Ni matrix contains numerous grain boundaries (GBs), which greatly enhance the effective diffusivities of the reactive elements for their selective oxidation at the onset of oxidation [18]. However, the inevitable microstructure evolution of the NC Ni matrix at high temperatures can decrease the supply of Cr and/or Al from the interior to the oxidation front, which would affect the steady-state growth of the chromia or alumina scale that has formed [18, 21]. Thus, understanding the thermal stability of NC Ni EDs at higher temperatures is helpful to develop chromia- and alumina-forming Ni-based NC coatings with desired long-term oxidation performance.

In this work, the thermal stability up to 800 °C of pure NC Ni EDs has been investigated in detail by DSC measurements coupled with surface analysis and microstructural characterization, with a focus on the DSC peaks at higher temperatures which have not caused much concern.

2 Experimental

2.1 Preparation for NC Ni EDs

NC Ni was electrodeposited onto a thin plate of copper or nickel from a nickel sulfate bath loaded with 150 g/l $NiSO_4{\cdot}6H_2O$, 15 g/l H_3BO_3, 15 g/l NH_4Cl, 0.1 g/l $C_{12}H_{25}NaSO_4$, and 1 g/l saccharin by a pulse reversal current (PRC) power with the parameters reported previously [22, 23]. The NC Ni EDs were ~ 70 μm thick. After being peeled off from the thin copper substrate, ~ 5 μm-thick Ni EDs were abraded from the deposit/copper interface side using SiC paper. Afterwards, the Ni EDs were rinsed using distilled water and ultrasonically cleaned in acetone for the compositional, microstructural, and calorimetric analyses. The NC Ni EDs have a mean grain size of 34 ± 12 nm based on the TEM characterization (Fig. S1 in Supplementary Material) and contain the impurities of 80 C, 880 S, 14 P, 110 O, < 50 Fe, and 100 Co (in ppmw) [24].

2.2 DSC Measurement

The calorimetric investigations were performed in a NETZSCH STA 449C instrument. The testing procedure method has been detailed in our previous works [22, 24] and is briefed here as follows. The DSC chamber was first pumped down to 10^{-2} Pa and then filled with high purity argon (99.999%) to 10^5 Pa. The pumping and filling processes were repeated 3 times. The temperature and energy were calibrated by use of pure In, Bi, Zn, Al, and Au. The Ni EDs with a weight of ~ 10 mg was placed in an alumina pan for testing. Non-isothermal measurement was conducted from room temperature to 800 °C at a scanning rate varied from 10 to 30 °C/min with an increment of 5 °C/min. After cooling down to room temperature at a cooling rate of 20 °C/min, a second run provided the DSC baseline for data analysis. Isothermal measurement was conducted for 5 h for part of the Ni EDs after heated up to a desired temperature at a rate of 30 °C/min. Flow of argon with a rate of 30 ml/min was kept all the time during the experiments.

2.3 Surface Analysis

For clarifying whether oxidation occurs or not, the Ni EDs after DSC test were further analyzed by A VG ESCALAB MK II X-ray photoelectron spectroscopy (XPS), with monochromatic Al Ka (1486.6 eV) radiation at a pass energy of 50 eV and a take-off angle of 90°. To minimize possible surface contaminations, an area of 2 mm × 2 mm of the Ni EDs after DSC measurement was preferentially sputtered for 15 s prior to the XPS analyses. The Ni EDs after cleaning were then depth-profiled at a sputtering rate of 0.2 nm/s to obtain oxidation information during DSC scan. For identifying the oxidation product which may occur at high temperatures in the atmosphere in the DSC chamber, the XPS spectra were also acquired from the Ni EDs after pre-annealed for a couple of hours at 1000 °C under high vacuum system (10^{-5} Pa) and then deconvoluted by using a commercial computer program (Eclipse provided by VG) using one or more Gaussian–Lorentzian shapes of peaks with fixed binding energy, and a Shirley background [25]. The deconvoluted peaks were identified by reference to an XPS data base [26, 27], or from compounds analyzed in the same apparatus.

2.4 Microstructrual Investigation

To understand evolution of the microstructure of the Ni EDs during DSC test, parallel tests for the NC Ni EDs sealed in quartz tubes under a pressure of approximately 10^{-2} Pa were conducted, with the same heating rate as the DSC measurements to the desired temperatures but quenched into water

for eliminating the heat effect during cooling on the EDs' microstructure. Two types of samples were prepared in quartz tubes. One is free-standing Ni EDs (with approximate dimensions of 10 mm × 10 mm × 60 μm) obtained after peeled off from Cu substrate with a surface area of 20 mm × 20 mm, which was used for bending and fractured cross-sectional characterization by scanning electron microscopy (SEM). The other one is deposited on Ni substrates with dimensions of 15 mm × 10 mm × 2 mm, which was used for surface characterization as well as microhardness test in the following section. Some samples of the Ni EDs with Ni substrate, after either being electrochemically etched in a nital solution (10% HNO_3 with balance being C_2H_5OH) at a voltage of 18 V for 30 s or chemically etched in a cupric sulfate solution (5 g $CuSO_4$ + 20 ml HCl + 20 ml H_2O) for 10 s, were investigated under SEM.

2.5 Microhardness Test

The Ni EDs with Ni substrates, both before and after the SEM observations, were used for microhardness test, by a WHW HV-1000 Vickers hardness tester with an applied load of 50 g and a dwell time of 10 s.

3 Results

3.1 DSC Scanning

Figure 1 shows the non-isothermal DSC curve of the NC Ni EDs (solid line) scanned from room temperature to 800 °C at a rate of 10 °C/min. It exhibits two exothermic peaks, P_1 and P_2. P_1 with the peak temperature at 290 °C has been extensively reported as the result of grain growth (including abnormal and normal grain growth) [13, 22, 24]. P_2, with an onset temperature of 340 °C, a peak temperature of 626 °C, and an end temperature of 745 °C, has been rarely reported. It is worth noting that the color of the Ni EDs starts to change after heating to the temperature higher than approximately 500 °C, from the metallic bright to grey. This, together with the calculated thermodynamic condition for oxidation of Ni (as provided in the supplementary materials), suggests that surface oxidation of the EDs occurs at higher temperatures. To confirm this, the as-deposited NC Ni EDs, after pre-annealed at 1000 °C for 2 h in a high vacuum system of approximately 10^{-5} Pa, was DSC scanned at the same heating rate. The result is presented by the dashed line in Fig. 1. A peak with its peak temperature of 650.2 °C is observed. Its generation releases an enthalpy of 9.9×10^3 J/mol, much smaller than that of P_2 (23.3×10^3 J/mol) in the curve without the pretreatment. The balance of the enthalpy is mainly released by its microstructure evolution such as grain growth. The assumption that the peak in the DSC curve with the annealing pretreatment arises from oxidation is also convinced by the SEM observation of the Ni grains of the EDs after the 2 h treatment at 1000 °C as shown in Fig. 2 (and its corresponding XRD result is shown in Fig. S2). The grains have already been coarsened to a micrometer-size range of 10.2 ± 4.3 μm, with which the microstructure evolution such as grain growth and/or recrystallization becomes impossible in the DSC scan to 800 °C (much lower than the pretreatment temperature of 1000 °C).

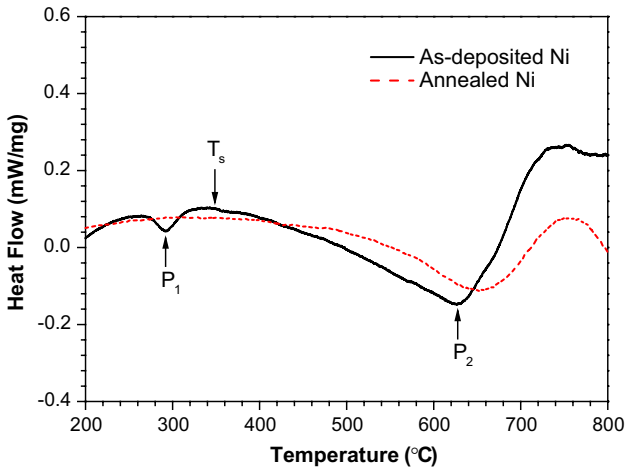

Fig. 1 DSC curves at a heating rate of 10 °C/min for the NC Ni EDs without (solid line) and with (dashed line) annealing pretreatment at 1000 °C in vacuum system (~ 10^{-5} Pa)

3.2 Microstructural Evolution During DSC Scanning

To better understand the effect of microstructure evolution of the Ni EDs on P_2 generation, evolution of the grain size of the NC Ni EDs after linearly heated at the rate of 10 °C/min to the temperatures close to its onset temperature, peak

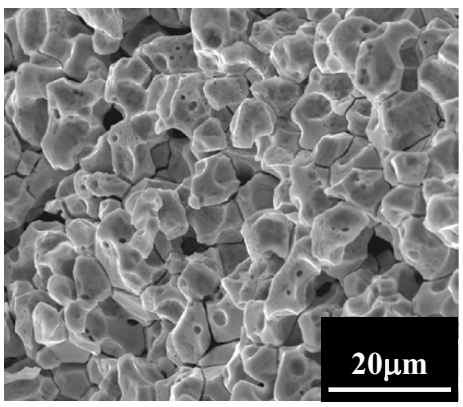

Fig. 2 Micrograph of the annealed Ni EDs after electrochemically etched in the nital solution

temperature, and end temperature, respectively, was investigated. Figure 3 shows SEM micrographs of the NC Ni EDs which were water quenched after being scanned to a temperature either lower or higher than the peak temperature. The mean size of the Ni grains at 345 °C (i.e., T_s in Fig. 1) is 476 ± 164 nm (Fig. 3a), which is comparable to that of 419 ± 148 nm observed by TEM (Fig. S3 in Supplementary Material) [24]. The Ni grains further grow to a mean size of 644 ± 208 nm at 600 °C, a temperature between the T_s and the peak temperature of P_2 (Fig. 3b). Intriguingly, the grain size in turn decreases to 550 ± 228 nm when the temperature rises to 640 °C, a temperature close to the peak temperature of the P_2 (Fig. 3c). This is credibly as a result of recrystallization of the NC Ni EDs. The recrystallization-induced grain-size decrease was also observed during annealing of Ni–P EDs [7]. Subsequently, the grains remain growing with increasing temperature. The size is 735 ± 243 nm at 650 °C (Fig. 3d). When temperature reaches 800 °C (much higher than the peak temperature), the recrystallized grains significantly grow to a size in a micrometer range, with a mean value of 1.77 ± 0.80 μm (Fig. 3e).

Figure 4 shows the fractured cross-sectional micrographs of the NC Ni EDs before and after heated to the various temperatures (some of their lower magnification micrographs are provided in Fig. S4). The as-deposited Ni exhibits columnar-like grains (Fig. 4a), which has been observed elsewhere [15]. The columnar-like grains are actually composed of numerous smaller equiaxed grains from an image in a higher magnification (Fig. 4b). The equiaxed grains are noticeably coarsened to a size of 475 ± 177 nm at 345 °C (Fig. 4c) and that of 663 ± 248 nm at 600 °C (Fig. 4d). Afterward, the Ni grains get smaller at

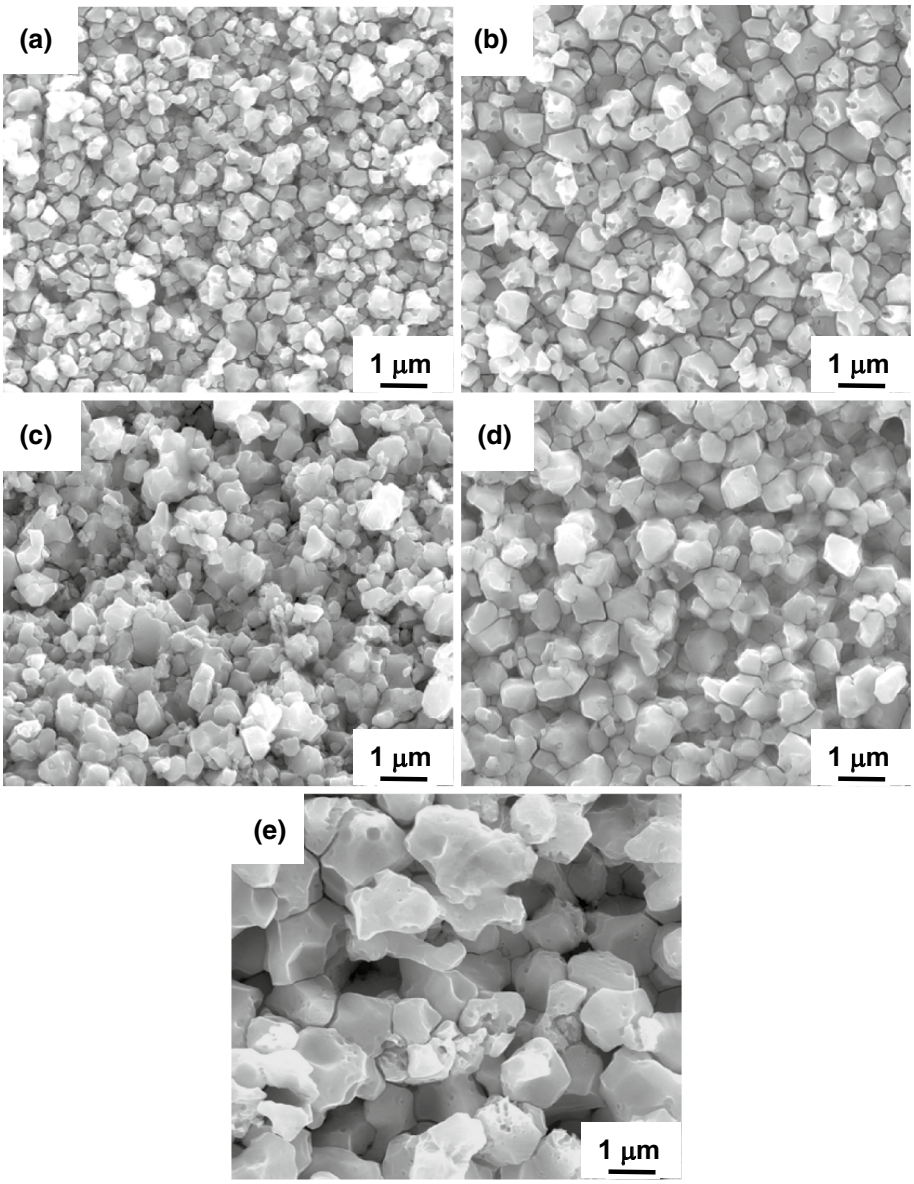

Fig. 3 SEM micrographs of the NC Ni EDs (etched in the nital solution) after linearly heated to **a** 345, **b** 600, **c** 640, **d** 650, and **e** 800 °C at 10 °C/min followed by water quenched to room temperature

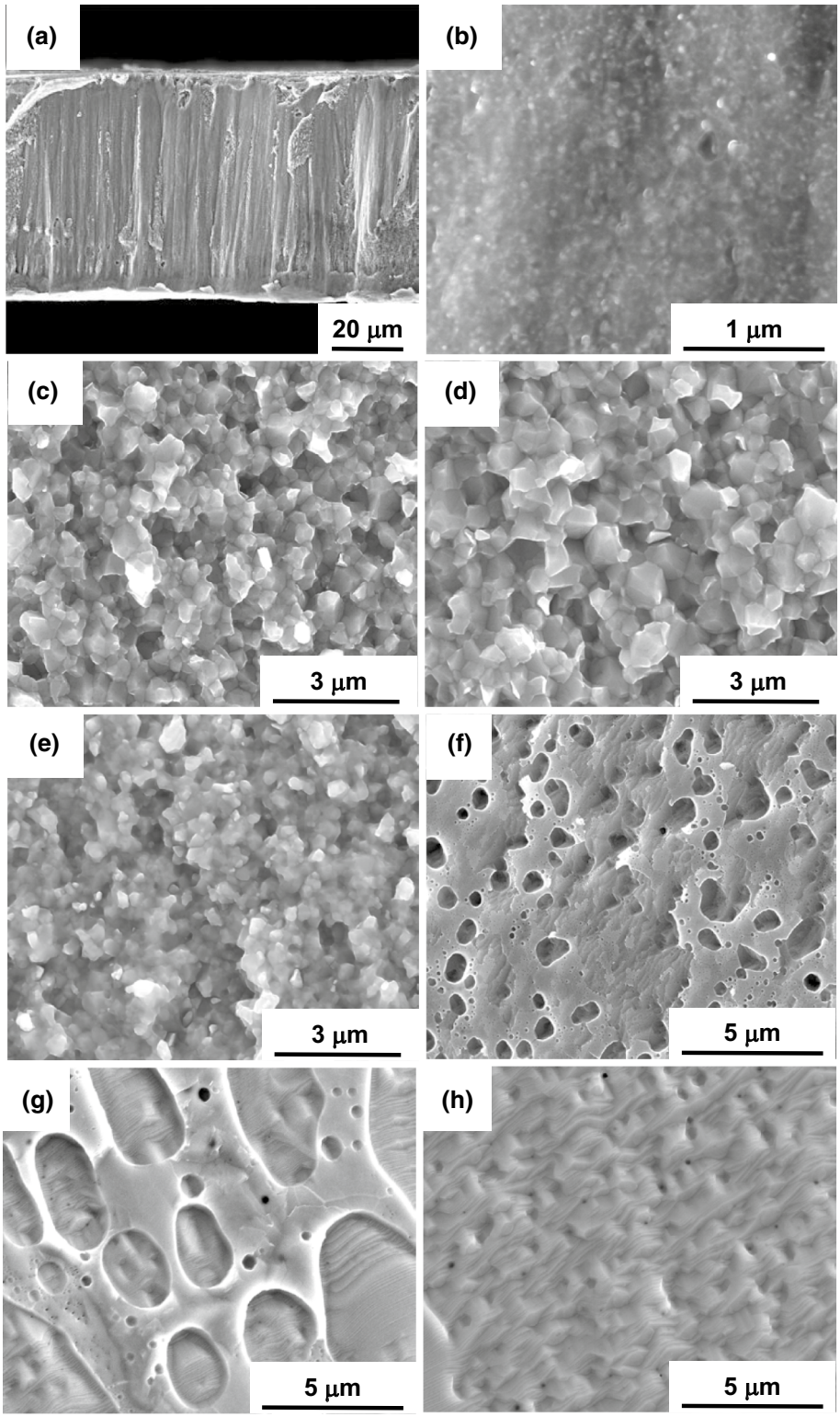

Fig. 4 Fractured cross-sections of **a, b** the as-deposited Ni and the deposits after heated to **c** 345, **d** 600, **e** 640, **f** 650, and **g**, **h** 800 °C at 10 °C/min followed by water quenched to room temperature

640 °C with the size of 404 ± 153 nm (Fig. 4e) due to the recrystallization of the Ni EDs as addressed above. In contrast, the Ni grains are not clearly seen at 650 °C; instead the Ni EDs display a feature with step-like striations and pores (Fig. 4f). Both the pores (Fig. 4g) and the striations (Fig. 4h) are further increased in size at 800 °C. The Ni grains in the typical cross-section can be disclosed by etching. Figure 5 and Fig. S5 show the etched cross-section of the Ni EDs after heated to 650 °C, the grain size of which is 759 ± 237 nm. Thus, the Ni grains after recrystallization

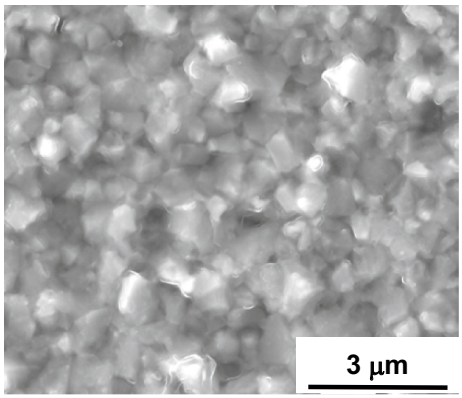

Fig. 5 Cross-sectional micrograph of the NC Ni EDs (etched in the cupric solution) after heated to 650 °C at 10 °C/min followed by water quenched to room temperature

grow very quickly, getting ~ 350 nm larger in size with an increase of 10 °C from 640 to 650 °C.

3.3 Mechanical Evolution During DSC Scanning

Figure 6 further shows the evolution of microhardness and grain size of the Ni EDs with increases in temperature. The hardness values were measured from the EDs, which were immediately quenched into water to room temperature after heated to the concerned temperatures. The as-deposited NC Ni has the microhardness of 498 ± 10 MPa. It gradually decreases with increase in the grain size to 644 ± 208 nm at 600 °C, but, sharply drops to only 96 ± 9 MPa in the temperature range 600–650 °C. Thereafter, the EDs' microhardness decreases gradually again. It was also found that the Ni EDs were easily fractured by bending before linearly scanned to 600 °C but difficult thereafter. This means that the Ni EDs experiences a transition in mechanical properties from brittle to ductile after 600 °C in the linearly heating process.

4 Discussion

4.1 Interpretation of P_2 Generation in DSC Scanning

4.1.1 Recrystallization Effect

Based on the results above, P_2 generation is intrinsically as the results of oxidation and recrystallization of the NC Ni EDs. For fully understanding the recrystallization contribution to the generation of P_2 in the non-isothermal DSC curve, isothermal DSC measurements of the NC Ni EDs were carried out in close proximity to the recrystallization temperature of 640 °C but using a heating rate of 30 °C/min, which is much faster than that for the non-isothermal DSC test to mitigate the heating process effect. Figure 7 displays two DSC curves during 5 h isothermal holding at 600 and 625 °C, respectively. A transition from the linear heating to the isothermal holding at approximately 20 min generates a sharp peak. An exothermic peak, which is not seen at 600 °C, occurs at 625 °C in the isothermal duration. Also, no exothermic peak can be observed in the isothermal duration for the annealed sample at 625 °C, as shown in Fig. S6. Thus, the exothermic peak is credibly from the recrystallization of the Ni EDs, which has been observed during the linear heating (Figs. 3, 4, 6). Recrystallization of NC Ni EDs was also reported by Talin et al. [5] and Suoninen et al. [6] during isothermal annealing, it occurred within 1 h but at a relatively lower

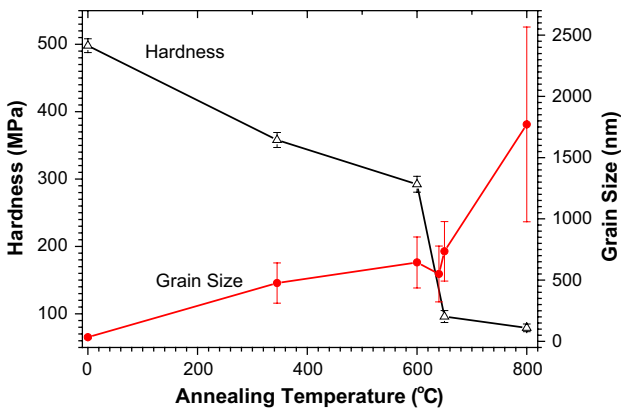

Fig. 6 Evolution of microhanrdness and grain size of the as-deposited Ni EDs with increasing temperature at 10 °C/min. The points at "0 °C" denote the cases without any annealing treatment

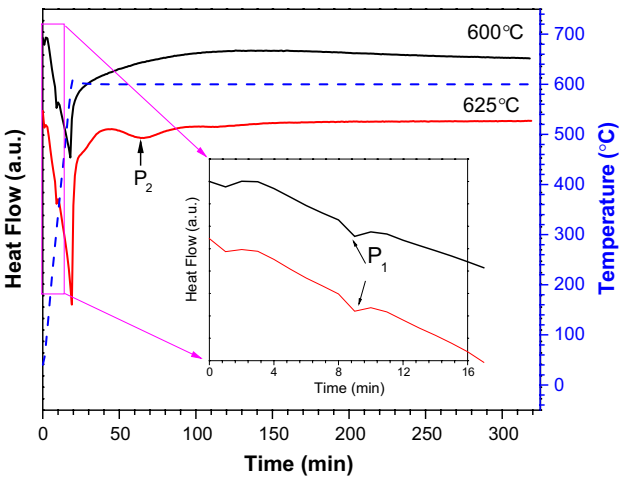

Fig. 7 DSC curves at a heating rate of 30 °C/min to 600 °C and 625 °C for 5 h, respectively, with the temperature indicated by the dashed line and P_1 in the heating stage indicated by the arrow in the inset

temperature (600 °C). One reason for the difference may be that different heating rate was used by them for the isothermal recrystallization testing which was not mentioned in their works. The other reason might result from that the as-deposited Ni EDs in [5, 6] and here are different not only in size, texture, and configuration of grains but also in the level of impurities (such as sulfur [5, 13, 24]), which also changes the energy for thermal activation of recrystallization.

Figure 8 shows the DSC curves during the 5 h isothermal holding at various temperatures of 625, 650, 664, and 675 °C, respectively. The time (t_p) for appearance of the peak decreases from 44.7, 33.5, 26.8, to 24.9 min with increasing temperature. If t_p is considered as that required time for 50% recrystallization ($t_{0.5}$), the relationship between t_p and the activation energy (Q) for recrystallization can be given using the following Arrhenius equation [28],

$$\frac{1}{t_p} = \frac{1}{t_{0.5}} = C\exp\left(-\frac{Q}{RT}\right) \quad (1)$$

where C is a pre-exponential factor. Taking Naperian logarithms of both sides of Eq. (1), the value of Q from the slope of the plot in Fig. 9 is calculated to be 85.7 kJ/mol.

The energy released by the recrystallization can be calculated according to the isothermal DSC holding. It is 7.8×10^3 J/mol from the DSC curve at 625 °C. This value is much lower than that of 23.3×10^3 J/mol from the non-isothermal DSC measurement because recrystallization only contributes partly to the generation of P_2 in Fig. 1.

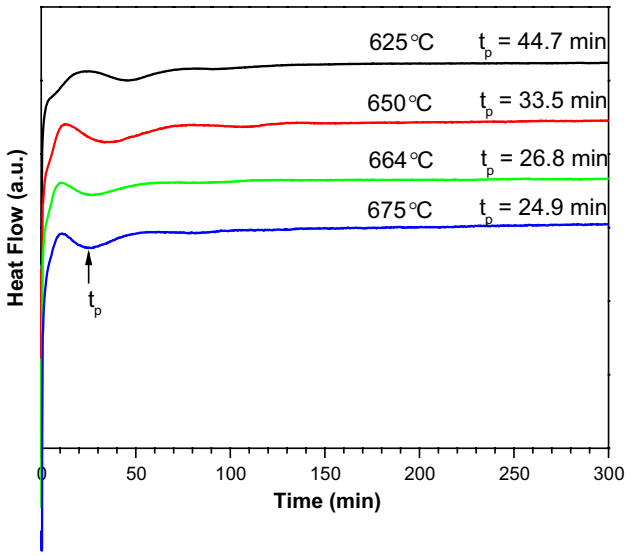

Fig. 8 Dependence of the generation of P_2 in the 5 h isothermal-scanning DSC curve on temperature

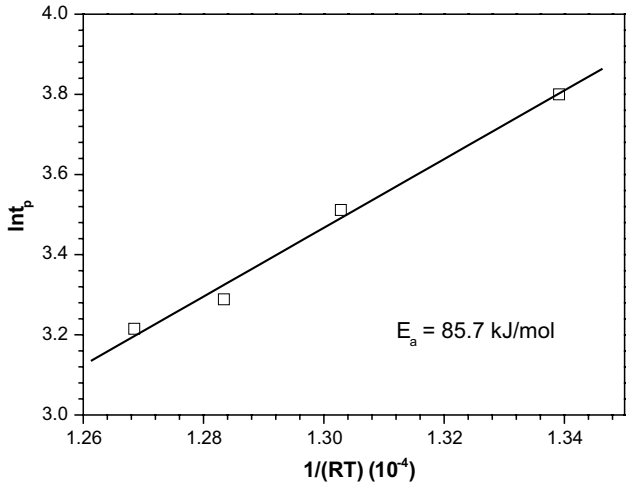

Fig. 9 Arrhenius plot of "Int_p" as a function of 1/RT

4.1.2 Oxidation Effect

The results have demonstrated that oxidation is the other factor which partly contributes to the P_2 generation. From the elemental XPS depth-profile in Fig. 10 of the NC Ni EDs after being scanned from room temperature to 565 °C at the rate of 10 °C/min, a ~200 nm-thick nickel oxide appears to grow on the EDs. Figure 11 shows a high-resolution XPS spectrum of the Ni EDs after scanned to 750 °C in the DSC chamber at the rate of 10 °C/min. The spectrum can be well deconvoluted by the standard spectra of NiO which has three "fingerprint" lines located at the binding energies of 854.6, 856.3, and 861.9 eV, and Ni which has two "fingerprint" lines at 853.0 and 858.0 eV. In addition, these XPS results

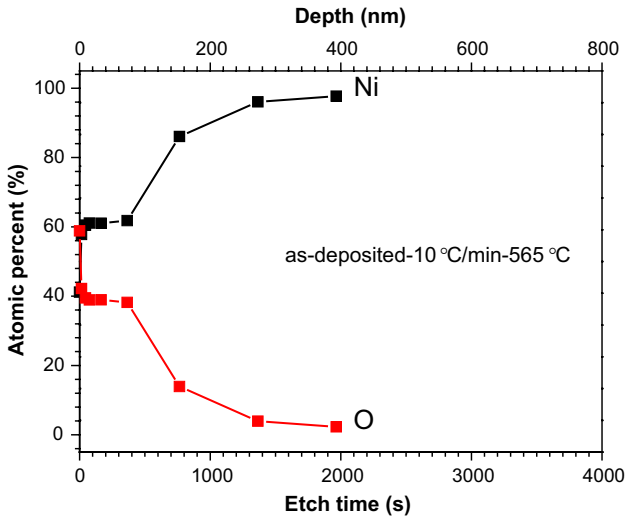

Fig. 10 XPS depth-profile of the NC Ni EDs after heated to 565 °C at 10 °C/min and then cooled to room temperature with the DSC chamber

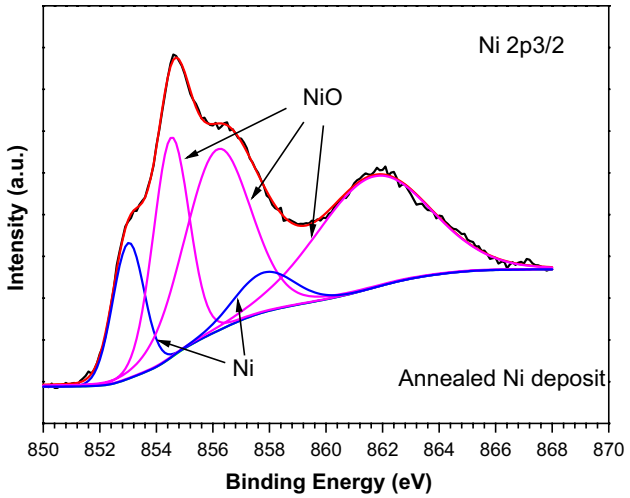

Fig. 11 XPS high-resolution spectrum of the NC Ni EDs after heated to 750 °C at 10 °C/min and then cooled to room temperature with the DSC chamber

indicate that the peak temperature for oxidation of the NC Ni EDs is apparently below 565 °C, implying that oxidation occurs prior to recrystallization (around 640 °C from Figs. 3, 4, 5) in the non-isothermal DSC scanning.

Thus, the P_2 of the as-deposited NC Ni EDs in the DSC scanning (Fig. 1) results from a superimposition of oxidation and recrystallization. It can be deconvoluted using two peaks as indicated by T_O and T_R in Fig. 12, one at a low temperature associated with oxidation and the other at a relatively higher temperature with recrystallization. The oxidation of the Ni EDs has a peak temperature of 541.8 °C and releases an enthalpy of 14.2×10^3 J/mol, and the recrystallization has a peak temperature of 635.9 °C and releases an enthalpy of 9.1×10^3 J/mol. The enthalpy by recrystallization is close to the value calculated from the isothermal DSC curve (7.8×10^3 J/mol).

By deconvolution of P_2 in the DSC curves at varied scanning rates of 10 °C/min to 30 °C/min, the peak temperatures of T_O and T_R are available. Accordingly, the activation energy (E_a) for oxidation and recrystallization of the NC Ni EDs can be calculated using Kissinger's equation as given by [29]

$$\ln\frac{B}{T_p^2} = -\frac{E_a}{RT_p} + C \tag{2}$$

where B is the scanning rate, and R is the gas constant. The result is presented in Fig. 13 and summarized in Table 1. T_p for the grain growth (i.e. the P_1 in Fig. 1) and E_a for oxidation of the annealed Ni ED are also presented for comparison. Recrystallization with respect to grain growth of the NC Ni EDs has lower activation energy but much higher released energy, suggesting that the EDs are easily recrystallized around appropriate temperatures. The activation energy for recrystallization obtained by non-isothermal DSC scanning (34.0 kJ/mol) is much lower than that by isothermal method (85.7 kJ/mol), plausibly due to that the 5 h isothermal holding at the high temperatures follows a heating process at a faster rate of 30 °C/min. The latter may decrease the stored energy in the grain boundaries of Ni EDs, which then makes their recrystallization more difficult. This is a reason that T_p for recrystallization increases with increasing heating rate (Table 1).

Here, it should be pointed out that oxidation of the Ni EDs occurs, even in the low oxygen partial pressure in the DSC processing atmosphere. This demonstrates that the NC Ni with respect to its conventionally coarse-grained counterpart has greatly increased in the susceptibility to oxidation. This can also be indirectly supported by the observations

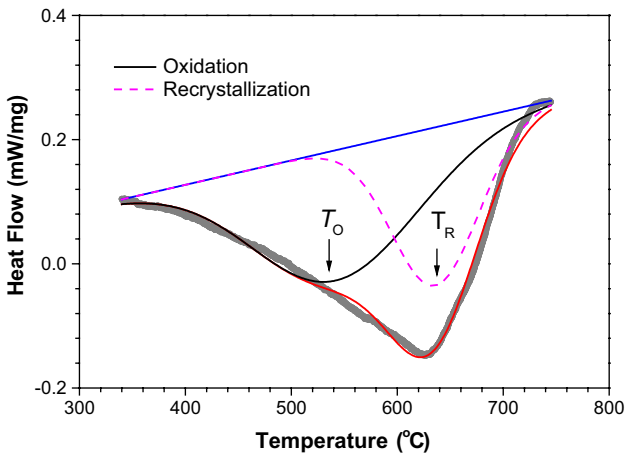

Fig. 12 Deconvolution of P_2 in the non-isothermal DSC curve (solid line) in Fig. 1

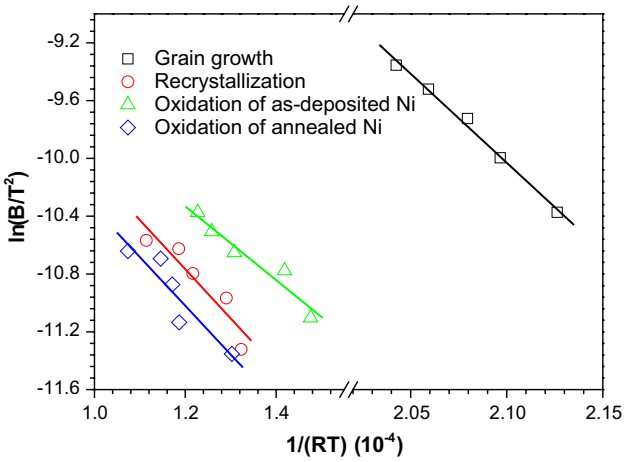

Fig. 13 Kissinger's plot of $\ln(B/T_p^2)$ versus $1/RT$ for the NC Ni EDs with and without annealing pretreatment

Table 1 Summary of DSC analysis results for the as-deposited and as-annealed Ni EDs: peak temperature (T_p), activation energy (E_a), and heat release ($\Delta H_{release}$)

	As-deposited Ni			As-annealed Ni
	Grain growth[a]	Recrystallization	Oxidation	Oxidation
T_p at 10 °C/min (°C)	292.5	635.9	541.8	650.2
T_p at 15 °C/min (°C)	300.5	658.9	574.8	740.5
T_p at 20 °C/min (°C)	305.2	715.4	646.4	753.7
T_p at 25 °C/min (°C)	310.9	741.3	682.8	776.6
T_p at 30 °C/min (°C)	315.7	806.2	706.8	846.9
E_a (kJ/mol)	138.8	34.0	25.5	33.7
$\Delta H_{release}$ (J/mol)	534.2	9.1×10^3	14.2×10^3	9.9×10^3

[a]The peak temperatures are from Ref. [23], as shown in Fig. S7

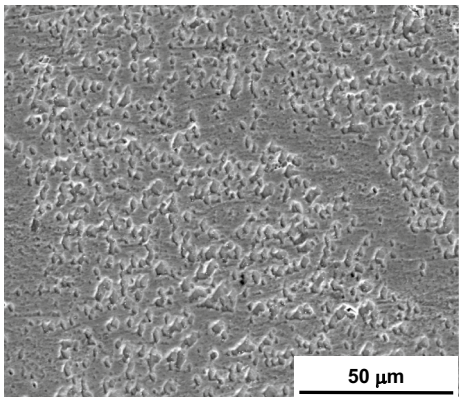

Fig. 14 Surface morphology of the NC Ni EDs after heated to 650 °C at 10 °C/min

that NC Ni EDs are oxidized faster than the coarse-grained counterpart [30, 31]. The former with respect to the latter has high surface energy and numerous grain boundaries, which promotes the nucleation and then growth of NiO at high temperatures.

4.2 Brittle–Ductile Transition in DSC Scanning

From the results above, growth of the grains of the NC Ni EDs with temperature can change their mechanical properties. After linearly heated to 650 °C at the rate of 10 °C/min in the DSC chamber, the Ni EDs are sharply decreased in hardness (Fig. 6). This undoubtedly results from their recrystallization, the peak temperature of which in the DSC scanning curve is 635.9 °C (Fig. 12). The generation of striations (Fig. 4f–h), a characteristic microscopic evidence of fatigue fracture driven by repeated or fluctuating stresses that are less than the tensile strength of the material [32], suggests that the Ni EDs are increased in ductility when they are heated up to the temperature above 600 °C. The brittle-to-ductile transition for the Ni EDs during heating is probably as the result of recrystallization, which leads to condensation of excess Ni vacancies in the interior of the Ni EDs to the surface. The condensation of the vacancies at the surface generates numerous cavities there, as seen in Fig. 14 and Fig. S8.

5 Conclusions

The NC Ni EDs with a mean grain size of 34 ± 12 nm generate a significant exothermic peak in the DSC curve in the range of 340–745 °C, during a linear heating process at the rate of 10 °C/min in a high purity Ar atmosphere. The peak occurs as a result of superimposed effects, i.e., recrystallization (a process including nucleation and subsequent growth of the newly formed grains) and surface oxidation of the Ni EDs. Oxidation appears to occur ahead of recrystallization. The temperatures for recrystallization and oxidation shift to higher values with increasing heating rate. The recrystallization leads to a sharp decrease in microhardness while increase in the ductility of the Ni EDs in a narrow range around the temperature initiating recrystallization. The results indicate that not only oxidation of the NC Ni EDs, even under a low oxygen partial pressure in the Ar atmosphere, is a considerable factor contributing to the generation of the exothermic peak in the non-isothermal DSC curve at elevated temperatures, but also the recrystallization can lead to the profound change of the mechanical property of the Ni EDs.

Acknowledgements The work is supported by National Natural Science Foundation of China (NSFC, project Grant No. 51271189).

Compliance with Ethical Standards

Conflict of interest All the authors declare that they have no conflict of interest.

References

1. H. Gleiter, Prog. Mater Sci. **33**, 223–315 (1989)
2. K. Lu, Mater. Sci. Eng. R Rep. **16**, 161–221 (1996)

3. C. Suryanarayana, Int. Mater. Rev. **40**, 41–64 (1995)
4. H. Gleiter, Acta Mater. **48**, 1–29 (2000)
5. A.A. Talin, E.A. Marquis, S.H. Goods, J.J. Kelly, M.K. Miller, Acta Mater. **54**, 1935–1947 (2006)
6. E.J. Suoninen, T. Hakkarainen, J. Mater. Sci. **3**, 446–448 (1968)
7. M.H. Seo, J.S. Kim, W.S. Hwang, D.J. Kim, S.S. Hwang, B.S. Chun, Surf. Coat. Technol. **176**, 135–140 (2004)
8. X. Zhou, Y. Shen, J. Mater. Sci. **49**, 3755–3774 (2014)
9. W. Chen, W. Gao, Compos. Part A Appl. Sci.Manuf. **42**, 1627–1634 (2011)
10. J.A. Desai, A. Kumar, Met. Mater. Int. **22**, 451–458 (2016)
11. M.J. Kim, J.S. Kim, D.J. Kim, H.P. Kim, Met. Mater. Int. **15**, 789 (2009)
12. G. Palumbo, D.M. Doyle, A.M. El-Sherik, U. Erb, K.T. Aust, Scr. Metall. Mater. **25**, 679–684 (1991)
13. U. Klement, U. Erb, A.M. El-Sherik, K.T. Aust, Mater. Sci. Eng., A **203**, 177–186 (1995)
14. N. Wang, Z. Wang, K.T. Aust, U. Erb, Acta Mater. **45**, 1655–1669 (1997)
15. C.-S. Lin, P.-C. Hsu, K.-C. Peng, L. Chang, C.-H. Chen, Mater. Trans. **42**, 316–322 (2001)
16. Y. Zhang, X. Peng, F. Wang, Mater. Lett. **58**, 1134–1138 (2004)
17. X. Yang, X. Peng, C. Xu, F. Wang, J. Electrochem. Soc. **156**, C167–C175 (2009)
18. X. Peng, Nanoscale **2**, 262–268 (2010)
19. X. Yang, X. Peng, F. Wang, Scr. Mater. **56**, 891–894 (2007)
20. C. Zhang, X. Peng, J. Zhao, F. Wang, J. Electrochem. Soc. **152**, B321–B326 (2005)
21. Y. Zhou, X. Peng, F. Wang, Scr. Mater. **55**, 1039–1042 (2006)
22. L. Zheng, X. Peng, F. Wang, J. Mater. Sci. **47**, 7759–7763 (2012)
23. L. Zheng, X. Peng, F. Wang, Chin. J. Mater. Res. **24**, 501–507 (2010)
24. L. Zheng, Z. Yang, H. Zhen, X. Peng, J. Mater. Res. **32**, 1741–1747 (2017)
25. D.A. Shirley, Phys. Rev. B **5**, 4709–4714 (1972)
26. J.F. Moulder, J. Chastain, R.C. King, *Handbook of X-ray Photoelectron Spectroscopy: A Reference Book of Standard Spectra for Identification and Interpretation of XPS Data* (Physical Electronics, Perkin-Elmer Corp, Eden Prairie, 1995)
27. J.L. Grosseau-Poussard, J.F. Dinhut, J.F. Silvain, R. Sabot, Appl. Surf. Sci. **151**, 49–62 (1999)
28. A. Rollett, F. Humphreys, G.S. Rohrer, M. Hatherly, *Recrystallization and Related Annealing Phenomena* (Elsevier, Oxford, 2004)
29. H.E. Kissinger, Anal. Chem. **29**, 1702–1706 (1957)
30. X. Peng, T. Li, W. Wu, Oxid. Met. **51**, 291–315 (1999)
31. X. Peng, D. Ping, T. Li, W. Wu, J. Electrochem. Soc. **145**, 389–398 (1998)
32. T.H. Courtney, *Mechanical Behavior of Materials* (McGraw-Hill, Boston, 2000)